Measurement of interstrip and coupling capacitances of silicon microstrip detectors

Conference Paper · December 1992

DOI: 10.1109/NSSMIC.1992.301193 · Source: IEEE Xplore

15 authors, including:

Nicolo Cartiglia

919 PUBLICATIONS **30,286** CITATIONS

SEE PROFILE

K. Yamamura

Hamamatsu

78 PUBLICATIONS **893** CITATIONS

SEE PROFILE

SCIPP 92/14
October, 1992

Measurement of Interstrip and Coupling Capacitances of Silicon Microstrip Detectors[1]

E. Barberis, N. Cartiglia, D. Hutchinson, J. Leslie,
C. LeVier, J. Rahn,W. Rowe, H.F.-W. Sadrozinski
Santa Cruz Institute for Particle Physics University of California, Santa Cruz, CA 95064
K. Yamamoto, K. Yamamura, Hamamatsu Photonics, Hamamatsu 435, Japan
T. Ohsugi, Hiroshima University, Higashi-Hiroshima 724, Japan
Y. Unno, KEK, Tsukuba 305, Japan
T. Aso, H. Miyata, Niigata University, Niigata 950-21, Japan
N.Tamura, Okayama University, Okayama 700, Japan

Abstract

We present a set of measurements of the capacitances on silicon microstrip detectors which are important for the operation of the detectors. Various strip widths on both the junction and ohmic side and widths of blocking p+ implant on the ohmic side have been implemented on test detectors. The interstrip, body and coupling capacitances of the strips were measured. The measured capacitances exhibit a strong frequency dependence. We have simulated with SPICE the resistive and capacitive network represented by the detectors and find good agreement between measurement and simulation. We have irradiated the detectors with ionizing radiation to test the radiation hardness of the design.

We have measured the noise increase induced in a fast low-noise amplifier due to the capacitive load of different strip geometries. The results agree with those obtained using discrete external capacitors.

I. INTRODUCTION

In typical silicon microstrip detectors with a pitch of 50 μm and thickness of 300 μm the interstrip capacitance is the largest contribution to the parasitic capacitance while the body (strip to backplane) capacitance contributes less than about 20%.

The total strip capacitance plays an important role since it contributes to the noise of the front-end amplifier.

The geometry of the strips has several consequences. We have pointed out before[1], that the interstrip capacitance can be minimized with narrow strip implants.

For the ohmic side where oxide charges tend to increase the interstrip capacitance, it is possible to decrease the interstrip capacitance with wide p-blocking strips[2]. In AC-coupled detectors, for fixed thickness of oxide and metal, the width of the strip implant determines the value of the coupling capacitance between the implant and the metal strip and therefore it has to be made large such that the signal collection in the amplifier is efficient. The width of the metal strip determines its resistance. This resistance is in series to the amplifier and has to be minimized in order to reduce the noise and the dispersion of the signal[3].

In this paper we describe the measurements of capacitances on AC-coupled test detectors of various geometries and simulations of the frequency dependence of the measurements. We also show the effect of ionizing radiation on the capacitance. Finally we verified our understanding of the capacitance of various strip width by measuring their effect on the noise of a fast amplifier-comparator chip.

II. EXPERIMENTAL SET-UP

We have measured both the interstrip and the body capacitance as a function of strip and p-blocking implant width. Test detectors were manufactured by Hamamatsu Photonics[4] to determine the optimal geometrical layout of double-sided silicon detectors for the SSC. They are single-sided sample detectors of 50 μm pitch and 5.88 cm length with either junction or ohmic side processing (Fig.1). The detectors are AC-coupled. The implant of each strip is connected to a bus through a 460kΩ polysilicon resistor and can be accessed via "DC" pads. The corresponding metal strip is isolated by a thin layer of silicon oxide and is connected to the "AC" pads on the other end. These two layers form the electrodes of the coupling capacitor and overlap almost completely except in the region of the DC pads. The biasing voltage can be supplied either from the detector backplane or using contact vias placed in the top plane.

Each sample detector is divided into 4 areas in order to offer different strip geometries. The four areas on the junction side contain different strip widths: 6μm, 10μm, 20μm, and 30μm. Three of them are serviced by the same bus and the fourth one (30 μm) is completely independent. For the ohmic side sample, the four zones correspond to different widths of the p+ blocking strips (6μm, 10μm, 20μm and 24μm), while the width of the n+ implant is kept constant for a particular detector at 6μm, 10μm or 20μm.

The measurements have been performed on both the AC and DC pads with a HP4284A LCR meter. We used the LCR meter in its "two terminals configuration": from the "high

[1] Work supported in part by the U.S. Department of Energy , the Texas National Research Laboratory Commission and the US-Japan Collaborative Program.

Presented at The IEEE Nuclear Science Symposium, Orlando, FL, October 27-31, 1992

terminal" a sine wave at a selectable frequency between 20Hz and 1MHz is sourced, passes through the device under test and is then sensed by the "low terminal". The LCR meter measures the attenuation and phase shift of the sine wave and from these two quantities it calculates the impedance. Before each measurement we have subtracted the stray capacitances

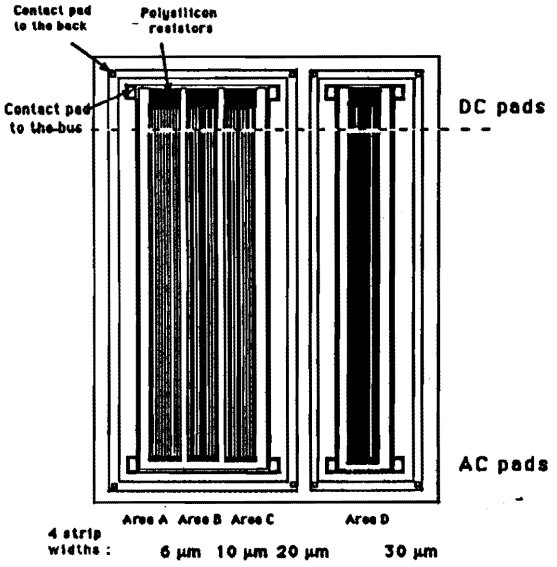

Fig. 1: Hamamatsu sample detector (p side).

due to cable loads and probes. The LCR meter can operate also in a "four terminals configuration"; both configurations gave identical results.

The terminals of the LCR meter were each connected through coaxial probes to one or several neighboring strips. Strips not directly used in the measurement but located close to the strips under test were grounded to avoid field distortions. The probe shields were connected among each other and to the system ground. We have measured the different contribution to the total interstrip capacitance due to the first neighbor, the 2 first neighbors, the 2 second neighbors, and all four neighbors. These different set-ups allowed us to check that the various contributions add up consistently. We have also measured the coupling capacitance by connecting the two probes to the AC pad and the DC pad of the strip, respectively.

During the measurements the detectors were biased at normal operating conditions (the p (n) implants were held at ground while the backplane was at 100 (-100) Volts.).

III. Frequency Dependence and SPICE Simulation

The experimental results show that the measured capacitance has a strong frequency dependence; this is especially true for the coupling capacitance. This result should not be surprising if we consider the detector as an extended network of resistors and capacitors. The p (or n) implant strip and the metal strip can be represented as a series of finite but small resistors with distributed capacitors to the other electrode, the neighboring strips and the backplane. The coupling capacitor shown in Fig.2 constitutes a low pass filter due to the high resistivity of the implant and leads to an apparent frequency dependence in the measured capacitance.

In order to extract the frequency independent capacitance per unit length, we have simulated our set-up and the LCR meter with the network simulator "SPICE".

We have divided the detector in unit cells , each consisting of two resistors for the top layer of aluminum and two resistors for the p+ implant. The resistance of the implant is about $4*10^3$ times larger than that of the metal. A coupling capacitor bridges the four resistors.

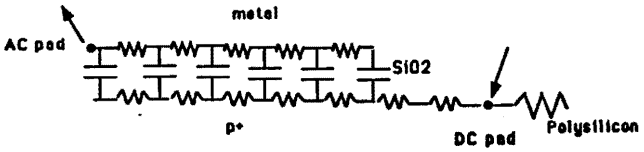

Fig. 2 Simulated detector using discrete components (coupling portion only).

The detector has been simulated by connecting the cells end to end and adding additional components (like the polysilicon resistors) at either end of the strip as shown in Fig.2. The number of resistors and capacitors per centimeter has been systematically doubled until there was no change in the shape of capacitance versus frequency curve. Convergence occurs for 64 cells per centimeter, corresponding to 128 resistors of each type and 64 capacitors. Since we determined that the contributions from the neighboring strips far removed are small, the simulated model contains five strips: one central and four neighbors. Each strip is capacitively coupled to the top layer of aluminum, the conductive backplane, its two closest neighbors and its two second neighbors.

The LCR meter was simulated by introducing a voltage source at the point corresponding to the location of the high probe and monitoring the current with an amperemeter placed at the position of the low probe. As mentioned above, the goal of the SPICE simulations is to extract a frequency independent capacitance and resistance from the frequency dependent measurement. A more complete description of the simulation and the results is given in Ref. [5].

IV. Results

A. Coupling capacitance

We have measured the coupling capacitance between the AC pad and the DC pad of the strip and we have obtained that

the results are independent on the biasing conditions of the detector.

The experimental and simulated results for the coupling capacitance are plotted in Fig. 3. The resistivity of the top aluminum layer has been measured directly but the design of the detector prohibits direct measurement of the p+ implant resistance, so SPICE was used to determine this value. The simulations agree very well with the data. The extracted coupling capacitance agrees with the low frequency limit of the measurement. At high frequencies (> 1KHz) only a small length of the p-implant contributes to the capacitance and thus the observed capacitance is reduced. The simulation also yields the value of the p+ implant resistance for each of the four strip widths.

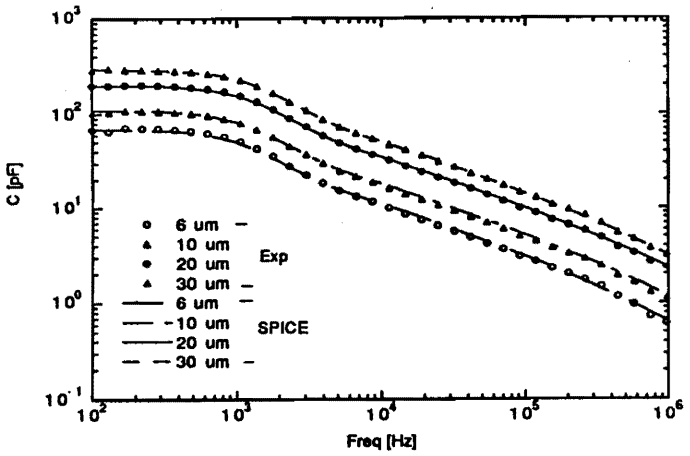

Fig. 3 Coupling capacitance (measurement and SPICE simulation) for different strip widths.

The values of the coupling capacitance per unit length and the resistance for the p+ implant are shown in Table1. Both the coupling capacitance and the implant resistance show good scaling with implant width.

Table I
Coupling Capacitance and p+ resistance

Strip width	p+ resistance	C/cm (pF/cm)
6 mm	670 KΩ/cm	11.9
10 mm	400 KΩ/cm	18.9
20 mm	200 KΩ/cm	34.1
30 mm	140 KΩ/cm	50.2

B. Interstrip capacitance

We have measured the interstrip capacitance using both the DC and AC pads of the detectors. Fig. 4a shows the probe placement and 4b the experimental and simulated results for the DC interstrip capacitance between one strip implant and its four next neighboring strip implants. Again, the agreement between data and simulation is good and the low frequency values essentially give the correct DC interstrip capacitance.

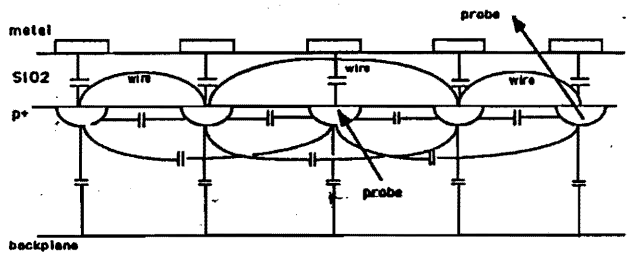

Fig. 4a: Probe placement for DC interstrip capacitance measurement

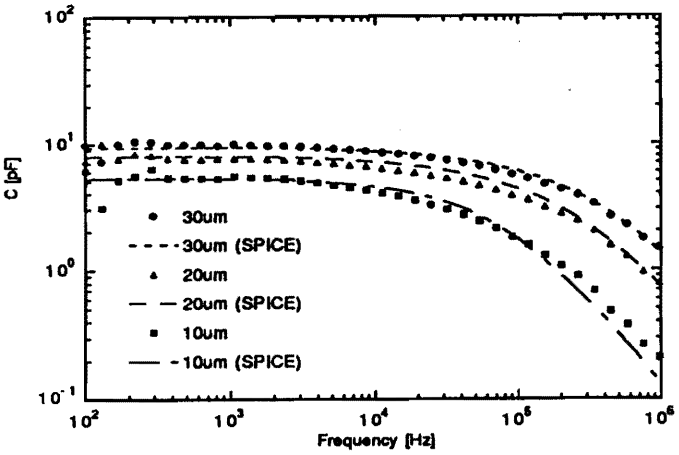

Fig 4b: DC interstrip capacitance (measurement and SPICE simulation) for different strip width.

Fig. 5a and 5b show the configuration and the results for the AC interstrip capacitance between one metal strip and its four next neighboring metal strips. Low frequencies are shunted to ground through the polysilicon resistors resulting in a high pass filter: the values for the AC interstrip capacitance extracted from SPICE are therefore close to the high frequency values of Fig 5b.

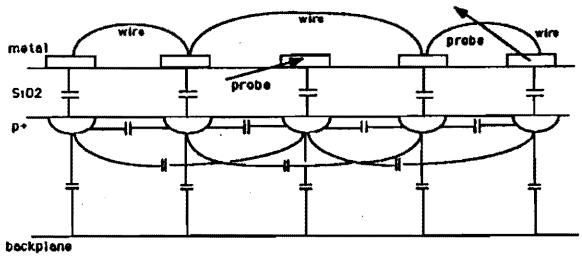

Fig. 5a: Probe placement for AC interstrip capacitance measurement.

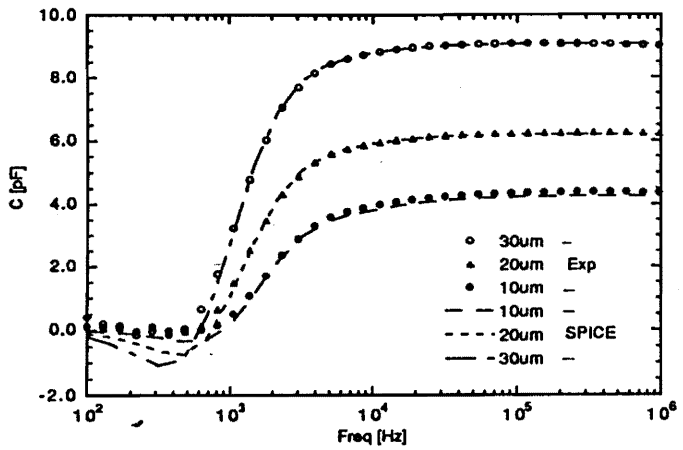

Fig. 5b: AC interstrip capacitance (measurement and SPICE simulation) for different strip width.

C. Body capacitance

We have measured the body capacitance of the whole detector placing one of the two terminals on the bus and the other on the backplane. The measured values agree with the estimate made considering the strip a parallel plate eapacitor with plate width equal to the strip pitch and the distance between the plates equal to the wafer thickness. This is 0.16pF/cm for 50 μm pitch, independent of the implant width.

D. Total capacitance

We have determined the total interstrip capacitance as the sum of the measured AC interstrip capacitance to the first 2 pairs of neighbors plus a small correction, 0.1pF/cm, due to the presence of all the remaining strips. This correction has been measured to be small since the coupling between strips decreases as their distance increases. The total capacitance is then the sum of the total interstrip capacitance and the body capacitance.

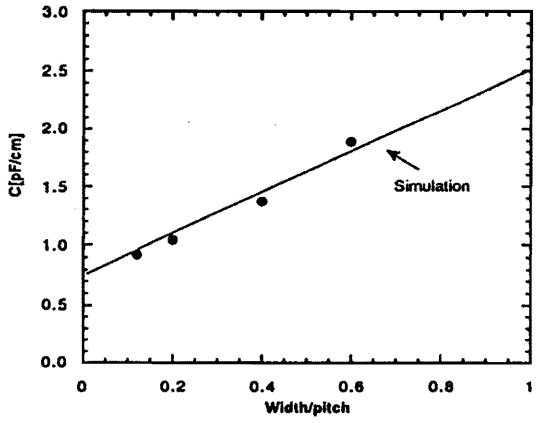

Fig. 6: Total capacitance for a 50 μm pitch p-side detector as a function of the ratio width/pitch.

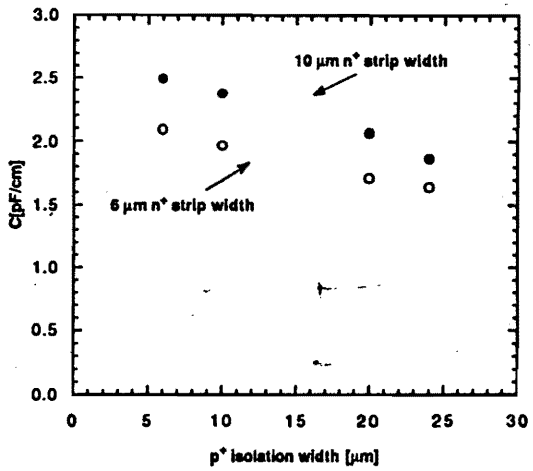

Fig, 7: Total capacitance for 50 μm pitch n-side silicon detectors for two strip widths as a function of p+ isolation width.

The total capacitance for p-side silicon detectors with different strip width but constant strip pitch (50 μm) is shown in Fig.6 as function of the ratio strip width over pitch. The results are compared with the theoretical prediction obtained solving numerically for the electric field inside the detector[1]. The measurement confirms our theoretical prediction that a reduced strip width lowers the total capacitance.

Fig. 7 shows the total capacitance for n-side detectors with 6 and 10 μm strip width as function of the width of the p+ blocking strip. For n-side detectors, wider p+isolation implants and narrower n-implants reduce the capacitance.

V. RADIATION DAMAGE

We have irradiated the sample detectors with gamma rays from a ^{60}Co source [6] with total doses of up to 5 Mrad.

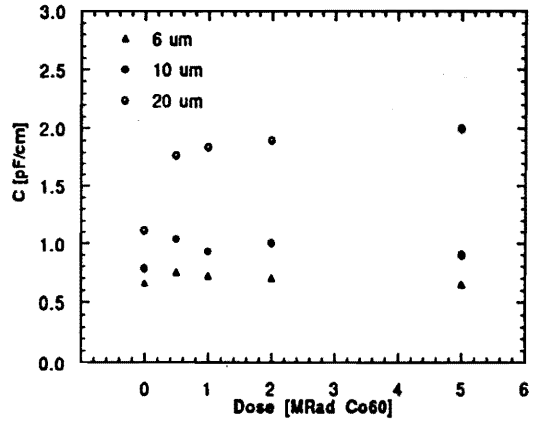

Fig. 8: p side interstrip capacitance to 1st and 2nd neighbors as a function of dose for different p+ strip widths.

During irradiation the backplane and the metal strip were held at ground while the p (n) implants were biased at -80 (+80) Volts.

We determined the AC interstrip capacitance for both the junction and ohmic side as a function of the total dose, choosing the high frequency limit at 1 MHz (cf Fig. 5b). The results are shown for the p side in Fig. 8 for different p-implant widths and in Fig. 9 for the n-side for different p+ blocking strip widths and n+ implant width of 10 μm. We find that detector geometries which give small capacitance, i.e. narrow strip implants and wide p+isolation, are also radiation hard. Larger strip width and narrower p+isolation show marked capacitance increases with irradiation. We have found before that the body capacitance does not change during irradiation[7].

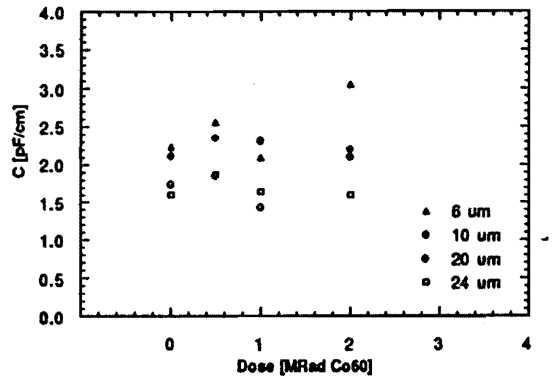

Fig. 9: n side interstrip capacitance to 1st and 2nd neighbors as a function of dose for 10 μm implant width for various p+ isolation widths.

VI. NOISE

The total strip capacitance plays an important role since it contributes to the noise of the front-end amplifier. This means that from a noise measurement we can deduce the input capacitance.One can ask the question if a complicated network like a detector behaves as a simple capacitative load. In order to answer this questions we have measured the noise of a low noise amplifier-comparator chip with 20ns rise time [8,9] with either discrete capacitors or silicon strip detectors of different width as load.

Fig.10 shows the noise of the amplifier as function of capacitance. In one case the capacitances were given by an external discrete component while in the other it was given by p-strips of different width, whose capacitance values can be taken from Fig. 6. The two noise curves are nearly identical. The finite resistance of the metal strip plays only a minor role because it is small enough.

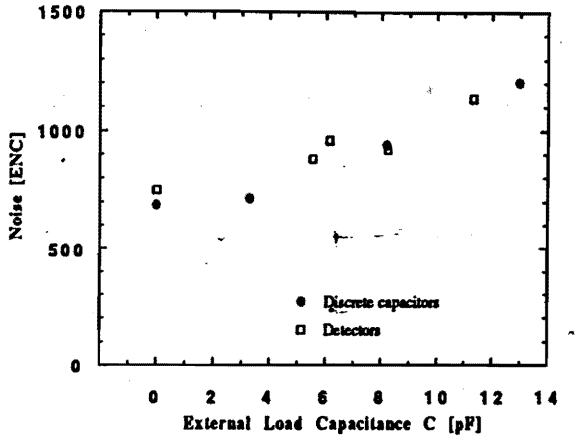

Fig. 10: Noise of an amplifier-comparator chip with 20 ns rise time as a function of load capacitance due to external discrete capacitors and total strip capacitances of different geometries.

VII. CONCLUSION

We have measured the parasitic and coupling capacitance of AC coupled silicon strip detectors. The frequency dependence of the measurement can be simulated with SPICE and is understood in terms of a network of distributed capacitors and resistors.

We found that the parasitic capacitances are minimized with narrow implant widths and wide p+ isolation strips. These geometries are measured to be radiation hard.

We have measured the noise of a fast low-noise amplifier as function of strip width and we have found that the results agree with those obtained with discrete components.

VIII. REFERENCES

[1] R. Sonnenblick et al., Electrostatic simulations for the design of silicon strip detectors and front-end electronics, Nuclear Instruments and Methods A310 (1991) 189.

[2] R. Yamamoto, Proceedings of the SDC Collaboration Meeting at KEK, SDC-91-33,May 1991.

[3] W. Gadomski et al., Pulse shapes of silicon strip detectors as a diagnostic tool,Contribution to the VIth European Symp. on Semiconductor Detectors,Milano,Italy, Feb. 1992, SCIPP 92/03.

[4] Hamamatsu Photonics K.K., Hamamatsu City, Japan.

[5] C. Levier, Capacitance in silicon strip detectors, UC Santa Cruz Senior thesis, SCIPP 92/26.

[6] H. Ziock et al., Trans. Nucl. Sci. 37, 1238 (1990)

[7] D. Pitzl et al., Type inversion in silicon detectors, Nuclear Instruments and Methods A311 (1992) 98.

[8] E. Barberis et al., A low power bipolar amplifier integrated circuit for the ZEUS silicon strip system, Contribution to the 3rd International Cinf. on Advanced Technology and Particle Physics,Como ,Italy June 1992, SCIPP 92/35.

[9] E. Barberis et al., A fast shaping amplifier/comparator integrated circuit for silicon strip detectors, IEEE Nuclear Science Symposium, October 1992, SCIPP 92/40.